ARMY RESEARCH LABORATORY

# Compact Femtosecond Pulse Approach to Explosives Detection Combining InN-Based Time Domain Terahertz Spectroscopy and Laser-Induced Breakdown Spectroscopy

**by Michael Wraback, Anand Sampath, and Dimitra Stratis-Cullum**

**ARL-TN-329** **August 2008**

## NOTICES

### Disclaimers

The findings in this report are not to be construed as an official Department of the Army position unless so designated by other authorized documents.

Citation of manufacturer's or trade names does not constitute an official endorsement or approval of the use thereof.

Destroy this report when it is no longer needed.  Do not return it to the originator.

**Army Research Laboratory**
Adelphi, MD 20783-1197

**ARL-TN-329** **August 2008**

# Compact Femtosecond Pulse Approach to Explosives Detection Combining InN-Based Time Domain Terahertz Spectroscopy and Laser-Induced Breakdown Spectroscopy

**Michael Wraback, Anand Sampath, and Dimitra Stratis-Cullum**
**Sensors and Electron Devices Directorate, ARL**

| REPORT DOCUMENTATION PAGE | Form Approved OMB No. 0704-0188 |
|---|---|



| 1. REPORT DATE *(DD-MM-YYYY)* | 2. REPORT TYPE | 3. DATES COVERED (From - To) |
|---|---|---|
| August 2008 | Final | October 2006–September 2007 |

**4. TITLE AND SUBTITLE**
Compact Femtosecond Pulse Approach to Explosives Detection Combining InN-Based Time Domain Terahertz Spectroscopy and Laser-Induced Breakdown Spectroscopy

**5a. CONTRACT NUMBER**

**5b. GRANT NUMBER**

**5c. PROGRAM ELEMENT NUMBER**

**6. AUTHOR(S)**
Michael Wraback, Anand Sampath, and Dimitra Stratis-Cullum

**5d. PROJECT NUMBER**
FY06-SED-02

**5e. TASK NUMBER**

**5f. WORK UNIT NUMBER**

**7. PERFORMING ORGANIZATION NAME(S) AND ADDRESS(ES)**
U.S. Army Research Laboratory
ATTN: AMSRD-ARL-SE-EM
Adelphi, MD 20783-1197

**8. PERFORMING ORGANIZATION REPORT NUMBER**
ARL-TN-329

**9. SPONSORING/MONITORING AGENCY NAME(S) AND ADDRESS(ES)**

**10. SPONSOR/MONITOR'S ACRONYM(S)**

**11. SPONSOR/MONITOR'S REPORT NUMBER(S)**

**12. DISTRIBUTION/AVAILABILITY STATEMENT**
Approved for public release; distribution is unlimited.

**13. SUPPLEMENTARY NOTES**

**14. ABSTRACT**
The feasibility of attaining improved explosives detection and identification using complementary InN-based time-domain terahertz spectroscopy (TDTS) and laser-induced breakdown spectroscopy (LIBS) techniques employing 1550-nm femtosecond (fs) pulse technology has been investigated. The use of very low-energy, ultra-short, near-infrared laser pulses for both TDTS and LIBS has been demonstrated. Novel approaches exploiting polarization fields in wurtzite nitride semiconductors such as InN and GaN led to an enhancement of THz generation by more than a factor of 3 relative to more conventional sources fabricated from these materials. These results could lead to improved THz sources at fs fiber laser wavelengths of interest, with further advances in material quality. Threshold LIBS pulse energies used in this investigation are the lowest reported to date, and gated detection is not required, potentially leading to an overall simpler and inexpensive system more amenable to field use. Finally, the use of low pulse energies in these studies currently available from more compact mode-locked fiber laser systems indicates potential for incorporation in field-deployable explosives-detection platforms.

**15. SUBJECT TERMS**
InN, terahertz, femtosecond, fiber laser, laser-induced breakdown spectroscopy, gated detection

| 16. SECURITY CLASSIFICATION OF: | | | 17. LIMITATION OF ABSTRACT | 18. NUMBER OF PAGES | 19a. NAME OF RESPONSIBLE PERSON |
|---|---|---|---|---|---|
| a. REPORT | b. ABSTRACT | c. THIS PAGE | | | Michael Wraback |
| UNCLASSIFIED | UNCLASSIFIED | UNCLASSIFIED | UL | 18 | 19b. TELEPHONE NUMBER (*Include area code*) 301-394-1459 |

**Standard Form 298 (Rev. 8/98)**
Prescribed by ANSI Std. Z39.18

## Contents

**List of Figures** **iv**

**Acknowledgments** **v**

**1. Objective** **1**

**2. Approach** **1**

**3. Results** **2**

3.1 Terahertz Studies ..... 2

3.2 Femtosecond LIBS studies ..... 5

**4. Conclusions** **7**

**5. References** **8**

**Distribution List** **9**

## List of Figures

Figure 1. Etched bars in nitride semiconductor with in-plane c-axis (top), and calculation of electric field in InN bars as a function of bar width (bottom). .....3

Figure 2. Terahertz radiation field amplitude as a function of sample rotation angle for nonpolar GaN samples with varying stacking fault densities (top). Conceptual band structure as a function of in-plane distance attributed to wurtzite material terminated by zincblende stacking faults (bottom). .....4

Figure 3. Compact 1580-nm fs fiber laser (top). THz data as a function of pump power showing minimum required power for system insertion of fs fiber laser (bottom). .....6

Figure 4. Atomic emission spectra of copper obtained by laser-induced breakdown of a clean copper sheet using 150-fs pulses from a tunable optical parametric amplifier. Spectra at various excitation wavelengths for pulse energy of 2 μJ, corresponding to fluence of 1.90 J/cm$^2$ (left). Pulse-energy-dependent spectra for 1400-nm excitation (right). Spectra were normalized to the peak intensity of the 521.94-nm emission line and offset for visual clarity. .....7

## Acknowledgments

The authors would like to thank Grace Metcalfe, Eric Readinger, and Alex Schill for terahertz measurements and analysis, InN and InN/InGaN multiple quantum well (MQW) growth and analysis, and laser-induced breakdown spectroscopy (LIBS) measurements and analysis, respectively. The authors would also like to thank Brad Arnold at the University of Maryland, Baltimore County, for the use of his amplified femtosecond laser LIBS facility and J. S. Speck at the University of California, Santa Barbara, for InN and InN/InGaN MQW samples.

INTENTIONALLY LEFT BLANK.

## 1. Objective

The objective of this research is to investigate the feasibility of attaining improved explosives detection and identification using complementary InN-based time-domain terahertz spectroscopy (TDTS) and laser-induced breakdown spectroscopy (LIBS) techniques employing 1550-nm femtosecond (fs) pulse technology. This technology can be potentially integrated in a compact, low-cost, field-deployable package based on fiber lasers/fiber optics.

## 2. Approach

Time-domain terahertz (THz) spectroscopy has recently been employed to measure the spectra of high explosives such as single-crystal HMX, RDX, and PETN (*1*). In spite of its potential, the THz regime remains one of the least-explored portions of the electromagnetic spectrum, in part because of the difficulty in efficiently generating and detecting terahertz radiation. One of the most successful approaches thus far for generation and detection of THz radiation uses optical pulses of ~100-fs duration to produce broadband radiation from semiconductors via acceleration of photogenerated charge, photo-Dember effect, and/or screening of internal electric fields. Traditionally, optically generated THz systems utilize fs mode-locked Ti-sapphire lasers or continuous-wave lasers with a wavelength near 800 nm. The large size and cost of these tabletop lasers, as well as the lack of operation in the 1550-nm spectral region suitable for compact fiber-based lasers, make the systems impractical for field deployment. The authors have been developing InN as a high-efficiency source of THz radiation because (1) its bandgap of ~0.65 eV (~1900 nm) (*2*) is compatible with generating THz radiation through above-bandgap excitation with either 1030- or 1550-nm compact fs fiber lasers and (2) it possesses a large spontaneous polarization that, when terminated at interfaces such as those found in multiple quantum wells, will create internal electric fields >1 MV/cm (*3*), more than 1 order of magnitude larger than those that can be created in traditional III-V arsenide and antimonide-based heterostructures. Since the maximum THz pulse energy is limited by the electrostatic energy stored in these effective nanocapacitors, and this energy is proportional to the square of the field, manipulation of these large internal electric fields using fs pulses should lead to significant enhancement in the efficiency of THz generation from these nanostructures.

Complementary information providing improved specificity in explosives detection can be obtained from LIBS, a form of analysis that uses emission generated from a laser-induced plasma to rapidly determine the elemental composition of a sample. Recent laboratory results (*4–6*) have shown that LIBS has great potential for explosives identification and could be

enhanced further if its elemental analysis could be combined with a complementary technique that provided molecular information, such as THz spectroscopy. Previous studies have shown improvements in LIBS sensor performance through the use of ultra-short laser pulses (ranging from 50 ps to hundreds of femtoseconds), compared to conventional 5- to 10-ns pulsed laser sources (*4*, *5*). A significant advantage of using ultra-short plasma generation includes reproducible sample ablation due to reduced thermal damage and lower threshold fluences of material ablation. These effects are largely attributed to the direct transition of material to the vapor or plasma phase without melting. For example, it has been previously shown that femtosecond excitation has several advantages over nanosecond excitation for spectroscopic plasma studies, including high precision of sample ablation, lower continuum background, and faster plasma dissipation, making possible the use of a nongated detector, provided that sufficiently high-peak irradiance intensities ($>10^{12}$–$10^{15}$ W/cm$^2$) are achieved. Despite the advantages of using ultra-fast laser pulses, the application of ultra-fast LIBS has not been practical due to the large size and costs associated with these types of laser sources.

Successful combination of the complementary TDTS and LIBS technologies for explosives detection using 1550-nm fs pulses will enable the replacement of the bulky tabletop spectroscopy systems by compact, low-cost fs fiber laser-based systems. These replacement systems would be field-deployable and predominantly eye-safe, except at the focus, which should be less of a problem for the envisioned remote automated systems employing fiber delivery.

## 3. Results

### 3.1 Terahertz Studies

In the first year of the program, successful generation of THz emission was demonstrated from bulk InN samples using fs pulses continuously tunable between 800 and 1500 nm. This work indicates that the efficiency of THz generation is inversely related to background carrier concentration. From a one-dimensional drift-diffusion model incorporating momentum conservation and relaxation, it was determined that the dominant mechanism for THz generation in bulk InN is the current associated with the diffusion of the photogenerated electrons at elevated electron temperature (photo-Dember effect) and the redistribution of the background electrons under drift (*7*). Subsequently, the authors designed and studied InN/InGaN multiple quantum wells (MQWs) from which THz radiation was generated. For 800-nm excitation, the ~2× enhancement of THz radiation from the InN MQWs relative to bulk InN can be attributed to the suppression of field screening by effectively localized background electrons in periodic triangular potential “wells” created by the piezoelectric and spontaneous polarization. For long wavelength excitation (up to 1700 nm), electron diffusion becomes less important, and the THz

signature from the MQWs is strongly influenced by electron drift in the barrier regions of the MQW due to the large polarization fields.

Building upon these results, a new concept was invented for enhanced THz radiation and output coupling using nitride semiconductor nanostructures with the internal electric field parallel to the sample surface. Such structures act as a contactless, higher-field analog to large-aperture photoconductive switches (figure 1). The added advantage of this configuration is that the THz radiation couples out of the structure ~5× more efficiently than for a vertical field, assuming the fs pulse has the 45° angle of incidence normally employed in these experiments. Such nanostructures might be fabricated from nonpolar a-plane or m-plane nitride semiconductors with the c-axis in-plane by terminating the spontaneous polarization using arrays of etched bars defined by e-beam lithography. While such structures have been realized, in doing so it was discovered that they were not necessary; that is, the same effect could be achieved without etching or e-beam lithography.

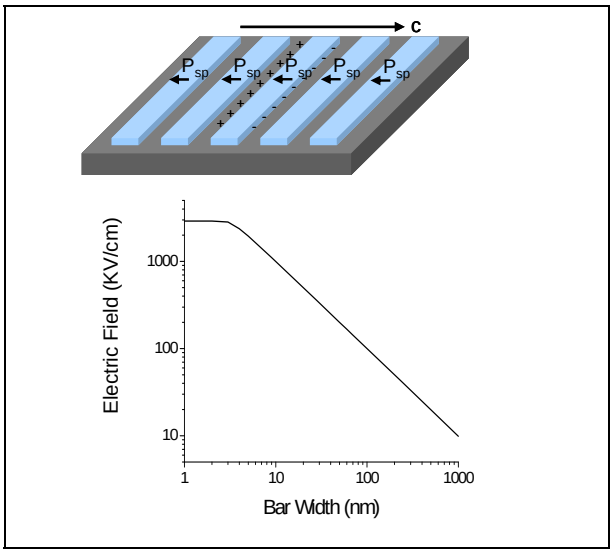


Figure 1. Etched bars in nitride semiconductor with in-plane c-axis (top), and calculation of electric field in InN bars as a function of bar width (bottom).

Figure 2 shows the THz emission amplitude from several nonpolar GaN samples with varying stacking fault densities as a function of sample rotation. These stacking faults result primarily from the large density of structural defects associated with heteroepitaxial growth on lattice-mismatched sapphire substrates. For comparison, a bulk nonpolar GaN substrate that should be nearly stacking fault-free is also included. The ZnTe-based THz electro-optic detection system is polarization sensitive, enabling analysis of the polarization of the THz radiation. Detection of both the vertical and horizontal components shows an oscillatory signal with 360° periodicity with respect to sample rotation. The vertical component is offset by 90° with respect to the

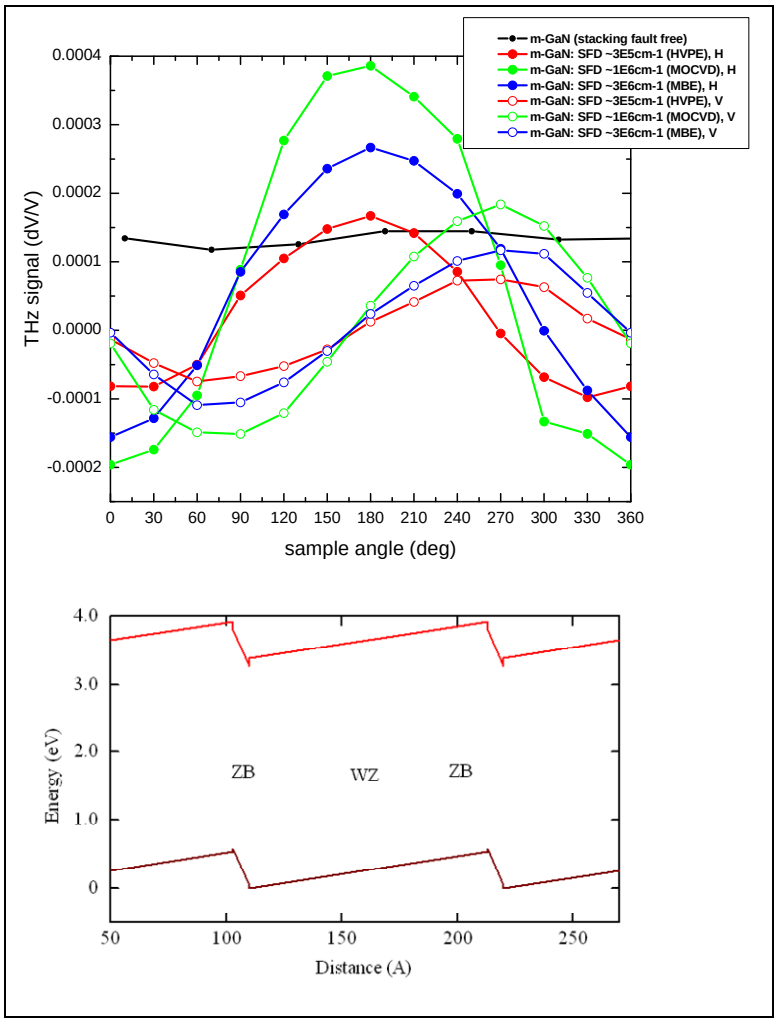


Figure 2. Terahertz radiation field amplitude as a function of sample rotation angle for nonpolar GaN samples with varying stacking fault densities (top). Conceptual band structure as a function of in-plane distance attributed to wurtzite material terminated by zincblende stacking faults (bottom).

horizontal component, as expected, and the horizontal component has an offset independent of rotation angle. The oscillation amplitude is very small for the stacking fault-free sample and increases significantly with increasing stacking fault density until the highest stacking fault density is reached, at which point the amplitude decreases again. These results suggest that the in-plane polarization of the wurtzite crystalline structure is terminated by stacking faults (*8*) that introduce thin zincblende domains of slightly lower bandgap, effectively creating in-plane MQW structures with strong polarization fields parallel to the c-axis of the crystal. In-plane transport of photoexcited carriers proceeds parallel to the polarization field, leading to THz radiation polarized preferentially along this axis of the sample. This mechanism provides the oscillatory

component of the THz amplitude as a function of sample angle. The offset observed for detection of the horizontal polarization emanates from the vertical, diffusion-driven carrier transport, which does not depend upon sample rotation. For stacking fault densities of ~3 $\times 10^5$ $cm^{-1}$, $1 \times 10^6$ $cm^{-1}$, and $3 \times 10^6$ $cm^{-1}$, the average spacing between stacking faults is 33, 10, and 3.3 nm, respectively, and the field increases with decreasing spacing in a manner similar to that shown in figure 1. The observation of a vanishingly small oscillatory component for the nearly stacking fault-free sample is consistent with this interpretation, as the in-plane field in this sample is expected to be small. The decrease in oscillation amplitude at the highest stacking fault density may be due to the higher background doping in this sample, although competing effects in the wurtzite and zincblende regions of the sample may also play a role, as they are expected to be of similar size and have opposite fields. Nevertheless, for an optimized stacking fault density, polarized THz radiation with an amplitude more than 3× larger than what one obtains from carrier diffusion alone can be generated from the nonpolar materials without any external processing. While this approach appears promising for enhanced generation of THz radiation from nitride semiconductors, it is important to note that significant challenges, including reducing background doping in InN and mitigating the surface electron accumulation layer on c-plane InN surfaces, still remain in extending this approach to InN-based structures for 1580-nm fs fiber laser pumping. However, InGaN structures that can be pumped with a frequency-doubled 1030-nm fs fiber laser are amenable to this approach and will be investigated.

A 1580-nm fs fiber laser was acquired and inserted into a THz spectroscopy system. This compact fiber laser (figure 3) produces ~100-fs pulses with ~50 mW of linearly polarized output power. Using an optical parametric amplifier (OPA) system, the minimum-required excitation power was measured to obtain a THz data trace. Figure 3 shows that data can be acquired for pump powers as low as 0.1 mW, which corresponds to ~16 mW of fs fiber laser power, taking into account the difference in laser pulse repetition rates. While this is well within the fs fiber laser power budget, a significant fraction of the fiber laser power will need to be used to detect the THz radiation. Possible detection approaches include electro-optic detection in GaAs at 1580 nm, frequency doubling and electro-optic detection in ZnTe at 790 nm, and GaAs photoconductive switches employing two-photon absorption. The authors are currently evaluating these alternatives while attempting to increase their options by decreasing detection noise through higher frequency modulation of the pump pulse. In addition, it was found that broadband-pulsed THz spectroscopy is effective in detecting and discriminating various types of explosive black powder and gun powder. Further details can be provided upon request.

### 3.2 Femtosecond LIBS studies

The main goals of the femtosecond LIBS studies have been to discern the emission, threshold, and continuum character of the low-energy plasma generation. While numerous studies have investigated the use of low-energy ultrashort laser pulses in micromachining applications, very little has been done to investigate the application of these pulses for use in LIBS. In order to

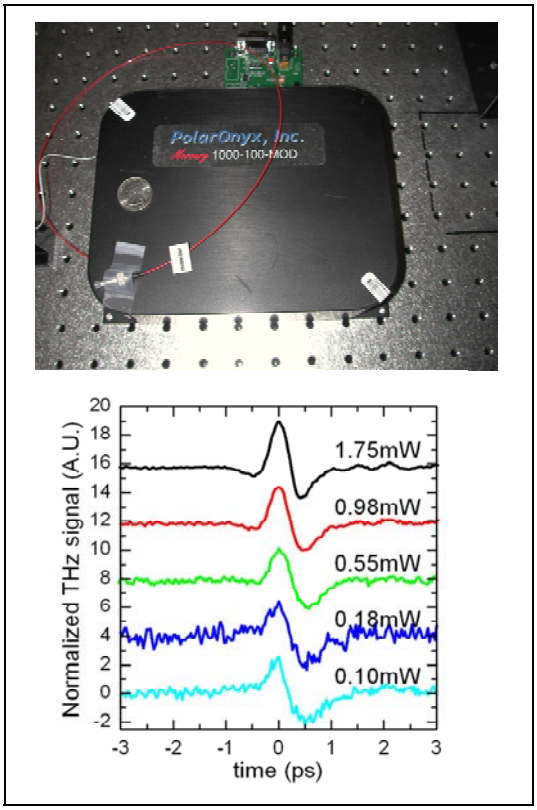


Figure 3. Compact 1580-nm fs fiber laser (top). THz data as a function of pump power showing minimum required power for system insertion of fs fiber laser (bottom).

investigate the use of ultra-short laser pulses that more approximate the wavelength region compatible with commercial fiber laser sources (i.e., 1–1.5 μm), studies were extended further into the near infrared (*9*). Figure 4 shows the emission spectrum of laser-induced plasma on the surface of a clean copper sheet using 150-fs pulses at three different near-infrared (NIR) wavelengths. The pulse energies were kept at 2 μJ, and all other experimental parameters were kept constant while the OPA was scanned from 1280 through 1420 nm. These data indicate that there is very little discernable difference in the spectra obtained using the three different pulse wavelengths, and that the apparatus does not introduce artifacts into the spectra at different pulse wavelengths.

The energy dependence of the plasma emission was then investigated to observe any differences in the threshold for plasma emission detection at these longer wavelengths. Shown in figure 4 are pulse-energy dependent emission spectra of copper for the longest wavelength investigated (1400 nm). It is clear that the pulse energies required for obtaining clean spectra (i.e., low continuum background) in a nongated mode are well below 2 μJ and were similar to those obtained during the first phase of this Director's Research Initiative using 785-nm laser

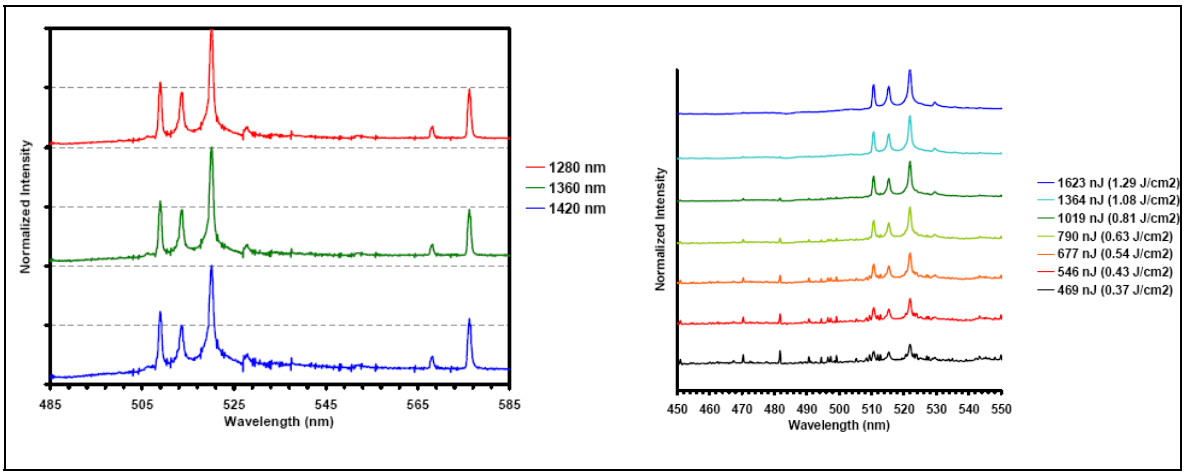


Figure 4. Atomic emission spectra of copper obtained by laser-induced breakdown of a clean copper sheet using 150-fs pulses from a tunable optical parametric amplifier. Spectra at various excitation wavelengths for pulse energy of 2 μJ, corresponding to fluence of 1.90 J/cm$^2$ (left). Pulse-energy-dependent spectra for 1400-nm excitation (right). Spectra were normalized to the peak intensity of the 521.94-nm emission line and offset for visual clarity.

pulses. This suggests that despite the low pulse energies (for the pulse width of the laser and irradiances used in this study), the plasma formation mechanism contributions from resonant absorption, multiphoton, and tunneling ionization occur in such a way that the initiation of the avalanche process and breakdown proceeds through effectively the same mechanism irrespective of the wavelengths investigated in this study. Moreover, although these studies were carried out on a metallic sample where resonant absorption is the dominant seed generation mechanism, it is expected that similar results will be observed in wide-band materials owing to effective multiphoton and tunneling ionization using ultra-short pulses.

## 4. Conclusions

The use of very low-energy, ultra-short NIR laser pulses for both TDTS and LIBS has been demonstrated. Novel approaches exploiting polarization fields in wurtzite nitride semiconductors such as InN and GaN lead to an enhancement of THz generation by more than a factor of 3 relative to more conventional sources fabricated from these materials. These results could lead to improved THz sources at fs fiber laser wavelengths of interest with further advances in material quality. Threshold LIBS pulse energies used in this investigation are the lowest reported to date, and gated detection is not required, potentially leading to an overall simpler and inexpensive system more amenable to field use. Finally, the use of low pulse energies in these studies currently available from more compact mode-locked fiber laser systems indicates potential for incorporation in field-deployable explosives-detection platforms.

## 5. References


1. Barber, J.; Hooks, D. E.; Funk, D. J.; Averitt, R. D.; Taylor, A. J.; Babikov, D. Temperature-Dependent Far-Infrared Spectra of Single Crystals of High Explosives Using Terahertz Time-Domain Spectroscopy. *J. Phys. Chem.* **2005**, *A109*, 3501.

2. Wu, J.; Walukiewicz, W.; Yu, K. M.; Ager, J. W., III; Haller, E. E.; Lu, H.; Schaff, W. J.; Saito, Y.; Nanishi, Y. Unusual Properties of the Fundamental Band Gap of InN. *Appl. Phys. Lett.* **2002**, *80*, 3967.

3. Bernardini, F.; Fiorentini, V.; Vanderbilt, D. Spontaneous Polarization and Piezoelectric Constants of III-V Nitrides. *Phys. Rev. B* **1997**, *56* (16), 10024.

4. Angel, S. M.; Stratis, D. N.; Eland, K. L.; Lai, T.; Berg, M. A.; Gold, D. M. LIBS Using Dual- and Ultra-Short Laser Pulses. *Fresenius' J. Anal. Chem.* **2001**, *369*, 320.

5. Eland, K. L.; Stratis, D. N.; Lai., T.; Berg, M. A.; Goode, S. R.; Angel, S. M. Some Comparisons of LIBS Measurements Using Nanosecond and Picosecond Laser Pulses. *Appl. Spectrosc.* **2001**, *55*, 279.

6. Rohwetter, Ph.; Yu, J.; Mejean, G.; Stelmaszczyk, K.; Salmon, E.; Kasparian, J.; Wolf J. P.; Woste, L. Remote LIBS With Ultrashort Pulses: Characteristics in Picosecond and Femtosecond Regimes. *J. Anal. At. Spectrom.* **2004**, *19*, 437.

7. Chern, G. D.; Readinger, E. D.; Shen, H.; Wraback, M.; Gallinat, C. S.; Koblmüller, G.; Speck, J. S. Excitation Wavelength Dependence of Terahertz Emission from InN and InAs. *Appl. Phys. Lett.* **2006**, *89*, 141115.

8. Majewski, J. A.; Vogl, P. Polarization and Band Offsets of Stacking Faults in AlN and GaN. *MRS Internet J. Nitride Semicond. Res.* **1998**, *3*, 21.

9. Schill, A. W.; Heaps, D. A.; Stratis-Cullum, D. N.; Arnold, B. R.; Pellegrino, P. M. Characterization of Near-Infrared Low Energy Ultra-Short Laser Pulses for Portable Applications of Laser Induced Breakdown Spectroscopy. *Optics Express*. **2007**, *15*, 14044.

NO. OF
COPIES ORGANIZATION

1 (PDF ONLY) DEFENSE TECHNICAL INFORMATION CTR
DTIC OCA
8725 JOHN J KINGMAN RD
STE 0944
FORT BELVOIR VA 22060-6218

1 DIRECTOR
US ARMY RESEARCH LAB
IMNE ALC IMS
2800 POWDER MILL RD
ADELPHI MD 20783-1197

1 DIRECTOR
US ARMY RESEARCH LAB
AMSRD ARL CI OK TL
2800 POWDER MILL RD
ADELPHI MD 20783-1197

1 DIRECTOR
US ARMY RESEARCH LAB
AMSRD ARL CI OK T
2800 POWDER MILL RD
ADELPHI MD 20783-1197

1 DIRECTOR
US ARMY RESEARCH LAB
AMSRD ARL RO EV
W D BACH
PO BOX 12211
RESEARCH TRIANGLE PARK
NC 27709

ABERDEEN PROVING GROUND

1 DIR USARL
AMSRD ARL CI OK TP (BLDG 4600)

INTENTIONALLY LEFT BLANK.